Machine-learning assisted handwriting recognition using graphene oxide-based hydrogel

Ying Liu[1,#], Fengling Zhuo[1,#], Jian Zhou[1,], Linjuan Kuang[1], Kaitao Tan[1], Haibao Lu[2], Jianbing Cai[1], Yihao Guo[1], Rongtao Cao[1], YongQing Fu[3], Huigao Duan[1]*

1. College of Mechanical and Vehicle Engineering, Hunan University, Changsha 410082, China.
2. National Key Laboratory of Science and Technology on Advanced Composites in Special Environments, Harbin Institute of Technology, Harbin, 150080, China.
3. Faculty of Engineering and Environment, Northumbria University, Newcastle upon Tyne, NE1 8ST, United Kingdom.

#These authors contributed equally to this work.

Corresponding Email: jianzhou@hnu.edu.cn

ABSTRACT： Machine-learning assisted handwriting recognition is crucial for development of next-generation biometric technologies. However, most of currently reported handwriting recognition systems are lacked in flexible sensing and machine learning capabilities, both of which are essential for implementations of intelligent systems. Herein, assisted by machine learning, we develop a new handwriting recognition system, which can be applied as both a recognizer for written texts and an encryptor for confidential information. This flexible and intelligent handwriting recognition system is composed of a graphene oxide-based hydrogel sensor and a printed circuit board, and offers a high sensitivity and a fast response time, allowing high-precision recognitions of handwritten contents from a single letter to words and signatures. By analyzing 690 acquired handwritten signatures obtained from 7 participants, we successfully demonstrate a recognition rate up to 91.30% and a recognition time of less than 1 s. Our developed handwriting recognition system has great potentials in advanced human-machine

interactions, wearable communication devices, soft robotics manipulators, and augmented virtual reality.

Keywords: handwriting recognition, hydrogel sensor, machine learning

1. INTRODUCTION

Handwriting recognition, which combines mathematical algorithms with advanced sensors to interpret handwritten contents, is crucial for the development of next-generation recognizers for written texts and encryptors for confidential information. Numerous studies have shown that the quality of data used in mathematical algorithms is one of the critical factors affecting the accuracy of intelligent recognition systems. [1-5] Recently, new types of flexible sensing techniques (e.g., stretchable sensors) have shown advanced applications in the field of intelligent recognition systems, which can overcome the shortcomings of rigid sensors and provide high-fidelity data acquisition.[6-11] Conducive hydrogels, which are crosslinked polymer networks infiltrated with water,[12] have recently emerged as promising materials for the fabrication of stretchable sensors due to their excellent electronic properties, tunable mechanical properties and remarkable biological characteristics.[13-16]

In recent years, many researchers have demonstrated that the conductive hydrogels can be applied as the sensing films for handwriting monitoring.[17-20] These conductive hydrogels can generate different voltage, current or resistance signals according to the differences in the forces, speeds, and sequences of the writing styles.[21-23] Based on these different signal characteristics, various handwriting contents can be distinguished for handwriting recognition. For example, Pan et al. fabricated an ionic-polyvinyl alcohol-tannic acid@talc supramolecular organohydrogel as a flexible keyboard for signature identification.[24] However, their hydrogels exhibit relatively low stretchability (with a maximum strain of 800%), thus limiting their application fields, especially those required for the hydrogels to tolerate mechanical deformations such as large stretching. Wang et al. proposed a crosslinked chitosan quaternary ammonium salt and liquid metal composite

hydrogel for handwriting detection.[25] However, the hydrogels show relatively low sensitivities (with a gauge factor of 1.6), which cannot accurately capture subtle movements during handwriting. Therefore, it remains a great challenge to develop a single hydrogel system that simultaneously integrates superior stretchability, high sensitivity and stability.

Stretchable sensing and machine learning technologies, two of the basic elements of an intelligent system,[26-30] can be effectively applied for the development of handwriting recognition system. However, the aforementioned studies were mainly focused on the acquisition of handwriting signals using hydrogel sensors, lacking the subsequent data analysis. As far as we have searched, there are two similar studies integrating machine learning technologies with hydrogel sensors to distinguish handwriting signals. Huang et al. proposed an integrated sensing system involving a hydrogel strain sensor for the handwriting recognition.[31] With the help of machine-learning algorithms, it could classify the finger joint's motion signals during the writing process. However, the accuracy of the machine learning model they adopted was only 75%. Similarly, Wu et al. integrated a machine learning module with the hydrogel strain sensor to achieve handwriting recognition by detecting finger movements.[32] However, their system has issues of low accuracy when used to recognize words with a high similarity. Instead of using hydrogels as the writing pads, the above studies achieved handwriting recognition by detecting finger movements during writing, but were limited in human-machine interface applications (e.g., drawing and playing electronic games). Therefore, it remains a great challenge to construct handwriting recognition system with a high recognition rate for various practical applications.

Herein, we develop a flexible handwriting recognition system using machine-learning assisted graphene oxide (GO) hydrogel sensor for high-precision signature recognition, in

which the GO hydrogel was reported in our previous study.[33] Multiple interpenetrating network architectures of GO hydrogels and strong interactions among components provide the sensing devices with excellent stretchability, high sensitivity and repeatability, thus enabling the acquisition of high-quality data. The resistance signals with different waveforms generated by the hydrogel sensors are converted into digital domains using the handwriting recognition system and machine learning technology. Our system offers fast recognitions of numbers, letters and words, owing to the powerful data analysis capability of the Bi-directional Long Short-Term Memory (BiLSTM) algorithm. To further illustrate the capability of signature recognition, a total of 690 handwritten signatures were acquired from 7 participants and successfully analyzed with the assistance of a machine-learning algorithm, demonstrating a high recognition rate of 91.30% and a short recognition time of less than 1 s. To demonstrate the prospects of the system in constructing human-machine interfaces, we successfully applied it to play the corresponding keys on a piano to generate different sounds.

2. HYDROGEL-BASED HANDWRITING RECOGNITION SYSTEM

The proposed intelligent handwriting recognition system consists of a GO hydrogel sensor and a printed circuit board (PCB). The fabrication of GO hydrogel was reported in our previous work.[33] The high sensitivity and good adhesiveness of the GO hydrogel sensor enable it to be conformably attached onto arbitrary and complex surfaces to accurately capture the information during the handwriting process, resulting in high-fidelity data acquisition. The PCB connected with the hydrogel integrates multiple functions, such as

signal conditioning and processing, using the available integrated circuit components. **Figure 1a** provides an overview of the process flow of the handwriting recognition system, including analog signal acquisition, conditioning and processing, all of which are integrated with a machine-learning algorithm for high-precision written recognition. **Figure 1b** illustrates the working principle of the BiLSTM model, demonstrating that the model is capable of processing and analyzing sequential data to improve the accuracy and efficiency of handwriting recognition system. The BiLSTM model is a combination of forward Long Short-Term Memory (LSTM) and backward LSTM models, which can assess information more accurately. The LSTM model can avoid long-term dependences, and its core idea is to add or remove information to the cell state through the designed "gate" structure.

The GO hydrogels were fabricated using the procedures reported in our previous paper.[33] In brief, GO, calcium chloride ($CaCl_2$), sodium casein (SC), and polydopamine (PDA) were integrated into a covalently crosslinked polyacrylamide (PAM) network, and multiple interpenetrating networks with multi-crosslinking of covalent bonds and non-covalent bonds were formed (**Figure 1ai**). The morphologies of the GO nanosheets that were utilized for the construction of electronic conductive pathways are shown in **Figures 1c** and **1d**, in which transmission electron microscope (TEM) and atomic force microscope (AFM) images indicate that the GO nanosheets were well exfoliated into 2D structures with an ultrathin thickness of ~1 nm. This paves the way for the efficient formation of conductive network in the hydrogel. **Figure 1e** shows the microstructural characterization of the freeze-dried hydrogel, which demonstrates an interconnected 3D porous network structure with a hierarchical pore size distribution.

Owing to the synergetic effects of multiple-network architectures and interactions, the resultant hydrogel reveals an excellent stretchability (**Figure S1**), which effectively extends the application range of our handwriting recognition system. The conductive

reduced GO (rGO) obtained from the partially converted GO through a PDA reduction process significantly enhances the electrical conductivity, resulting in an electronic-ionic hybrid conductive hydrogel with a high strain sensitivity.[33] This high sensitivity is crucial for the precise capture of subtle movements during the handwriting. The strain sensitivity of the hydrogel was determined by calculating the gauge factor (GF, where high value means higher sensitivity) from the slope of the relative resistance change ($(R - R_0)/R_0$) versus strain curve. **Figure 1f** shows that the relative resistance changes of the hydrogel sensor are increased with the tensile strains and can be split into two linear responsive regions, e.g., 0–1000% with a GF of 4.58 (R^2 =0.9787) and 1000–2000% with a GF of 9.98 (R^2 =0.99468). The response mechanism can be summarized as the 3D network structure transformation of the rGO nanosheets embedded within the hydrogel matrix. Within a narrow strain range and at an early stage, relative displacements occur among the rGO nanosheets, but free electrons are still able to pass through the breakpoints of conductive networks according to the tunneling effect, thus leading to a small resistance change and a low value of GF. With the increase of strains, the entire conductive network can be disintegrated as a result of the continuous expansion of rGO nanosheets' spacings, thus resulting in significant blocking of electron transmissions. A sharp rise of the resistance and an increased GF can thus be achieved. Compared with other material systems, the GO hydrogel sensor not only exhibits a high sensitivity in a large strain range (e.g., 2,000%), but also performs well in a narrow strain range (Figure S2). The mechanical durability is an important characteristic of the GO hydrogel sensor for long-term usages in practical applications. We investigated the cyclic stability of the hydrogel sensor, which was subjected to 1200 stretching-releasing cycles (100% strain, 200 mm/s). The obtained signal outputs are shown in **Figure 1g**, which reveals a reliable cyclic stability with a slight increase of resistance. The unique structural design ensures that the hydrogel maintains high sensitivity, excellent stretchability and robustness when used as a sensing film for

handwriting recognition.

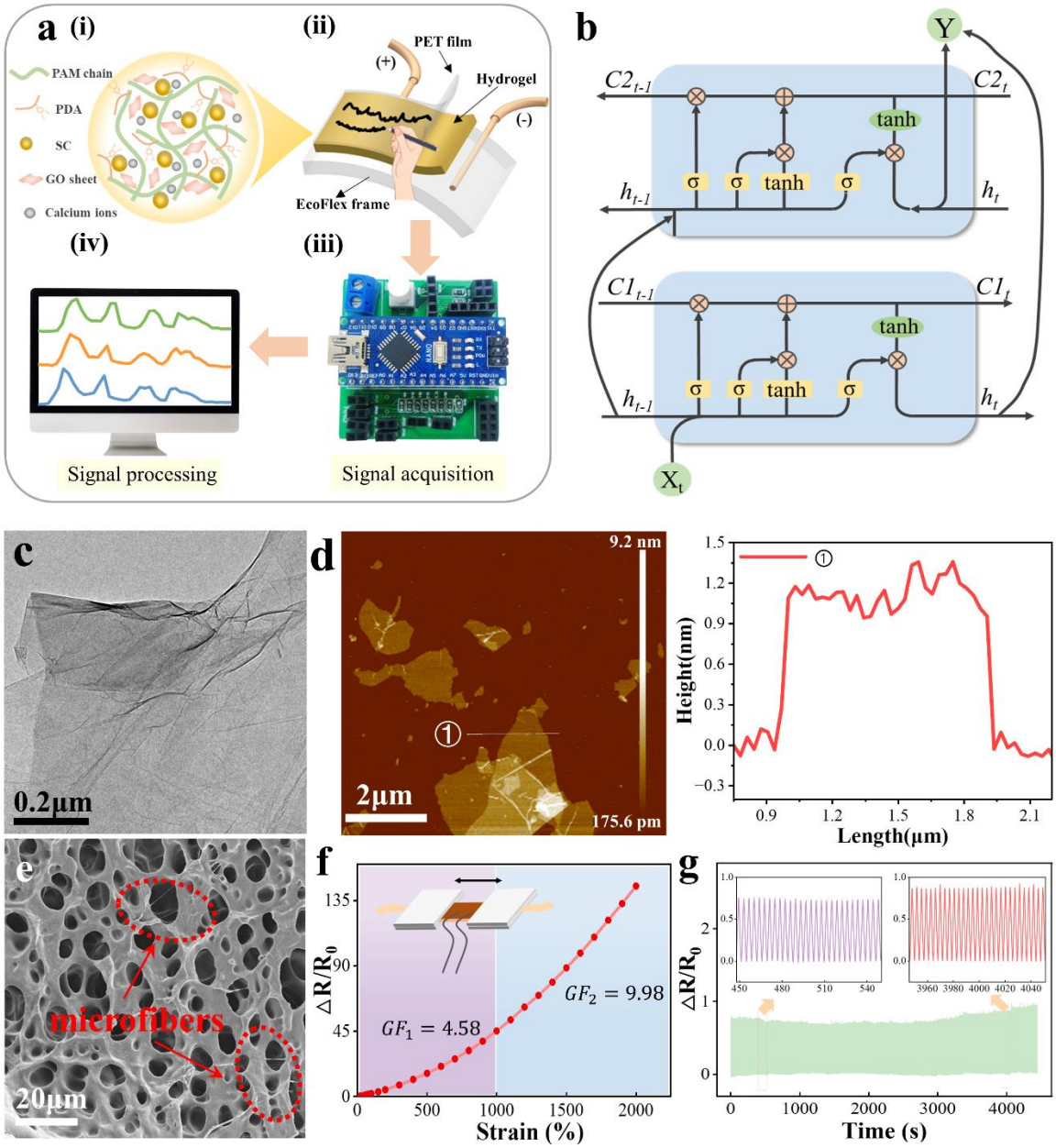

Figure 1. Schematic illustrations of the handwriting recognition system, together with the characterization and performance of the GO hydrogel. (a) Schematic illustrations of the handwriting recognition system; (b) Schematic diagram of BiLSTM model; (c) Transmission electron microscopy (TEM) image and (d) atomic force microscope (AFM) image of GO nanosheets; (e) Scanning electron microscope (SEM) morphology of the GO

hydrogel; (f) $\Delta R/R_0$ value of the GO hydrogel sensor versus the applied strain; (g) Durability test of the GO hydrogel sensor over 1200 cycles (100% strain).

3. DATA COLLECTION AND CLASSIFICATION PERFORMANCE

Owing to the high sensitivity, excellent stretchability and self-adhesiveness of the conductive hydrogels, the assembled system can be comfortably attached to various surfaces for high-precision written stroke recognition. In this work, to demonstrate the capability of hydrogel-based handwriting signal acquisition, the performance of the hydrogel in response to the pressing force of the pen tips was firstly evaluated. The GO hydrogel was sandwiched between an Ecoflex frame and a polyethylene terephthalate (PET) film, which can protect the hydrogels from mechanical failure and reducing friction of the pencil during writing.

A flow diagram of the machine-learning process using the conductive GO hydrogel sensor is shown in **Figure 2a**. During the training process, the resistance data generated by the hydrogel sensor are input into a matrix as the source of BiLSTM model, which is used to classify the handwriting signals. The machine learning algorithm sets each class of the acquired handwriting content as a classifier sample, and realizes the handwriting recognition by training the created classifier. During the signature recognition, a similar flow diagram is applied. The difference is that the datasets used for training and recognition are different, i.e., different handwriting contents.

To implement a recognition task on the hydrogel system, 36 common words were written on the hydrogel to represent the fundamental elements of the handwriting recognition categories—26 letters and 10 numbers. We built a custom letter-dataset containing 2,600 handwriting samples distributed into 26 categories of English letters from “A” to “Z”, and a custom number-dataset containing 955 handwriting samples distributed into 10 categories of numbers from “0” to “9”. **Figure 2b** shows the resistance signals obtained from the hydrogel sensor corresponding to handwritten letters, during which

pressure amplitude, writing speed, and motion tracking all show influences on the intensities and patterns of output signals. In general, writing pressure/amplitude and writing speed affect intensity and density of the output signals, respectively, while motion tracking affects patterns of the output signals. **Figure S3** shows effects of these parameters on the intensities and patterns of output signals. The output reliability of the hydrogel sensor was ensured by a continuous repetition of each handwriting—at least 55 times for each status (**Figure S4**). Similarly, the resistance data curves corresponding to handwritten numbers are shown in **Figure 2f**. Thus, each motion status of the handwritten contents can be reliably expressed as electrical signals from the hydrogel sensor.

To verify the performance of handwriting recognition system, different machine learning methods have been used to analyze the collected handwriting signals after preprocessing. These include the Logistic Regression (LR), Decision Tree (DT), Support Vector Machine (SVM) and K-Nearest Neighbors (KNN) classifiers, as well as deep convolutional neural networks (CNN). By employing different convolution kernels, CNN can automatically derive the correlation features and reduce the data complexity for handwriting classification. Sparse categorical accuracy is used to evaluate the performance of different algorithms in handwriting recognition system. The recognition accuracy rate of the CNN model is as high as 94.66%, which is similar to the KNN model (85.77%) but superior to the SVM model (67.50%), indicating that CNN model performs better in analyzing data from hydrogel sensors (**Figure S5**).

We further implemented four common neural network structure models for handwriting recognitions. **Table 1** lists the comparison of various parameters for the operation results of the four neural network models (i.e., LeNet-5, AlexNet, VGG16 and ResNet) and the CNN model (**Figure S6**). Experimental platforms and hyperparameters of different models are provided in the supporting information (**Table S1-S5** includes all these data). The accuracy (ACC) and loss curves were obtained to compare the recognition

abilities of these approaches. The training time was used to evaluate the responsiveness of these methods. Our results clearly show that compared to the results of several machine learning and common neural network models, the proposed CNN model offers the best performance in terms of accuracy, loss value and training time.

Considering that the obtained data are sequential data, we further explored the performance of our dataset in some typical recurrent neural networks, including Recurrent Neural Network (RNN), LSTM, gated recurrent unit (GRU) and BiLSTM. **Table 1** shows the comparison results of various parameters (e.g., Accuracy, Loss, Val_accuracy, Val_loss and Time/sample) of different models for recognizing 26 letters. In order to obtain the optimal model, apart from comparing the values of each parameter listed above, we also compared their training processes (e.g., trend of parameter curve, convergence speed and generalization performance of the model). The obtained results are presented in **Figure S7**. The results clearly show that the BiLSTM model outperforms the CNN model in all the dimensions, therefore, we finally adopted the BiLSTM model instead of the CNN model for the hydrogel handwriting recognition system. The high classification accuracy is attributed to the high-quality data collected by the GO hydrogel sensor and the usage of improved algorithm (i.e., BiLSTM).

Our applied custom letter dataset include 26 categories of letters, each of which contains 100 samples. The dimensions of each sample are different, with a maximum value of 106 and a minimum one of 10. In order to facilitate operations such as feature extraction, the dimensions of all samples are unified to 64, and the empty part is filled with the last value of each sample. Meanwhile, to make the model easier to converge and shorten the training time, it is necessary to normalize the samples of the dataset. We used the maximum-minimum normalization method to linearly transform the data and mapped the data to the [0,1] interval in this study, as shown in **Equation 1**.

$$x' = \frac{x - min(x)}{max(x) - min(x)} \qquad (1)$$

Three-quarters of the processed data were then randomly selected from the acquired signals as the training set, and the rest of the signals were applied as the test set. The obtained accuracy and loss curves for recognizing 26 letters and 10 numbers are shown in **Figure 2c** and **2g**, and the recognition accuracy values of the BiLSTM model reach 96.97% and 92.80%, respectively. The confusion matrices of these two classification results are presented in **Figures 2d** and **2h**, respectively. Each row of the matrix represents the test samples in an actual class, while each column represents a predicted class. Additionally, as shown in **Figures 2e** and **2i**, we used t-distributed stochastic neighbor embedding (t-SNE, a dimensionality reduction technique) to visualize the information within each sample group for the custom 26 letter-dataset and the 10 number-dataset, respectively. Each point on the plot represents the information of one handwriting projected from the 64-dimensional data to two-dimensional one. The points of the same letter or number category (or the same color) are clustered together, forming roughly 26 categories of letters and 10 categories of numbers (**Figure S8**). These results suggest that handwriting information on the hydrogel sensor can be served as valuable information for handwriting recognition system, which can be completely distinguished using machine-learning mechanisms.

Table 1 Comparisons of 26 letters recognized by different convolutional neural network and some typical recurrent neural network models

Model	Loss	Accuracy	Val_loss	Val_accuracy	Time/sample
LeNet-5	1.04908	0.59519	1.09341	0.58269	243us
AlexNet	0.26879	0.91875	0.69495	0.77308	4ms
VGG16	0.3713	0.85192	0.21716	0.90769	20ms
ResNet	0.07819	0.98462	0.12907	0.97308	14ms
CNN	0.13444	0.94664	0.15653	0.95962	107us
RNN	0.277201	0.885096	0.118656	0.957692	43us
LSTM	0.141603	0.945673	0.106445	0.95	80us
GRU	0.218448	0.921154	0.076037	0.959615	67us
BiLSTM	0.081692	0.969712	0.050336	0.980769	85us

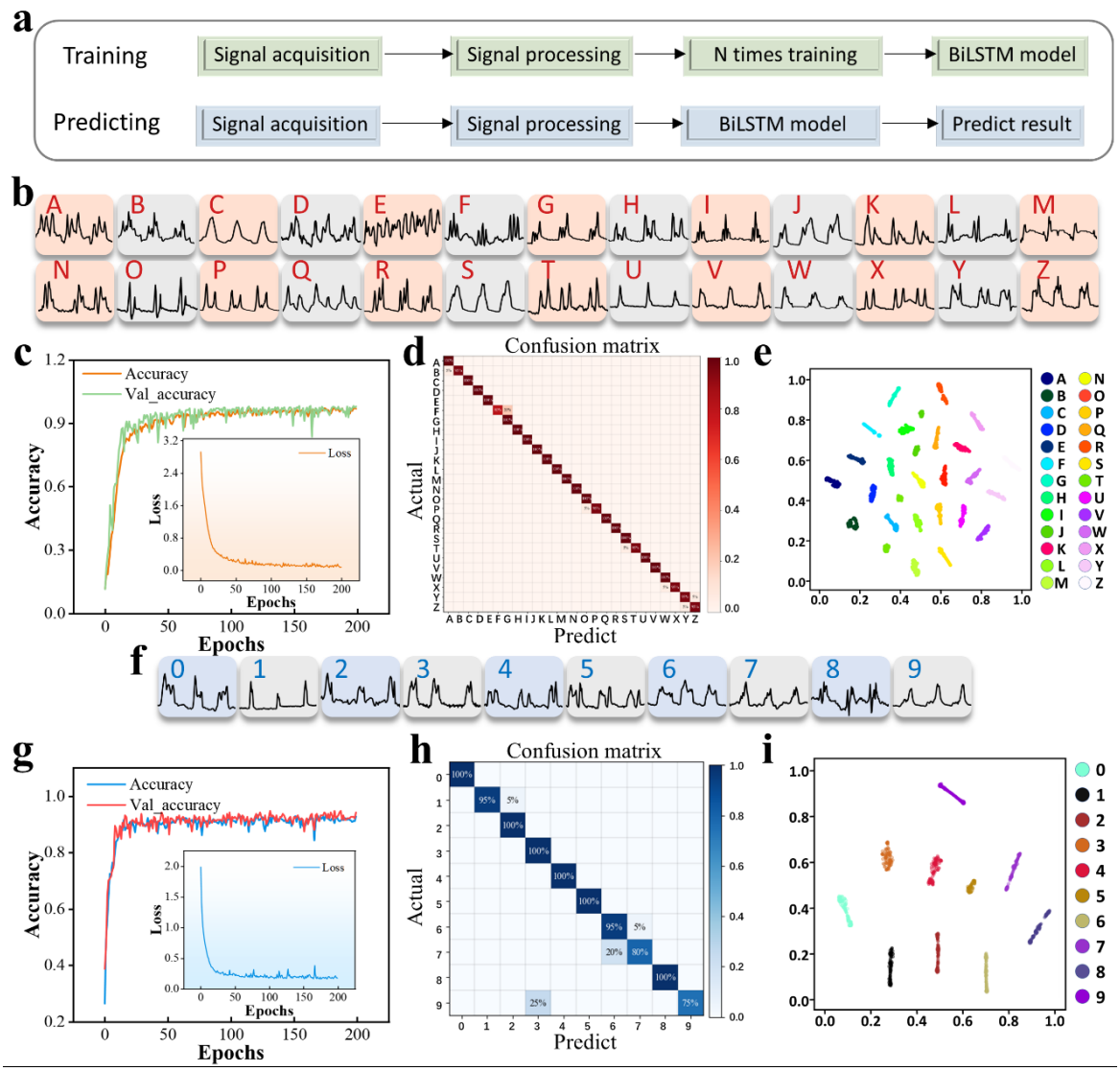

Figure 2. Recognition of letters and numbers. (a) The data process flow of the hydrogel handwriting recognition system, including a training process and an actual recognition process. **(b)** Resistance changes in response to handwriting 26 letters **(c)** Accuracy and loss curves for recognizing 26 letters. **(d)** Confusion matrix for recognizing 26 letters. **(e)** Visualizing the information within the 2,600 samples in the dataset using t-SNE dimensionality reduction. **(f)** Resistance changes in response to handwriting 10 numbers. **(g)** Accuracy and loss curves for recognizing 10 numbers. **(h)** Confusion matrix for recognizing 10 numbers. **(i)** Visualizing the information within the 955 samples in the

dataset using t-SNE dimensionality reduction.

4. DEMONSTRATION OF THE HANDWRITING RECOGNITION SYSTEM

To further optimize the performance of the hydrogel-based handwriting recognition system, we input a series of slightly different words into the system to verify the recognition effect, and the results are presented in **Figure 3**. These slightly different words can be divided into three categories: (1) the words with a sequential transformation; (2) the words with a letter addition; and (3) the words with a letter replacement. We conducted these experiments to demonstrate its ability to distinguish subtle differences among similar words. Taking the groups of “bare” and “bear”, “forth” and “fourth”, “altar” and “alter” as typical examples, we customized 100 sets of data for each group of words. After a series of processing and parameter adjustment, the accuracy and loss curves achieved the desired prediction results with an accuracy of approach 90%, as shown in the **Figures 3a-c**. Such a high accuracy provides a great potential for recognizing similar words using the machine learning algorithms. **Figures 3e-g** show the confusion matrixes, demonstrating the good performance of the handwriting recognition system for recognizing each type of word group.

In addition, it's common to replace one letter in a word to change into totally different words. For recognizing these similar words, we took examples and wrote “file”, “nile”, “mile” and “rile” on the hydrogel to collect the corresponding data. After processing the signals, we divided the training set and the test set with a ratio of 4:1, and then performed the training process. The obtained results in **Figure 3d** show that the accuracy reaches 90%, which is an ideal result for the recognition of similar words in multiple classifications. **Figure 3h** shows the confusion matrix with extremely high values on the diagonal, indicating that our handwriting recognition system has a high accuracy in recognizing similar word groups. The above experimental results show that the developed handwriting recognition system performed well in distinguishing the subtle differences among similar

words.

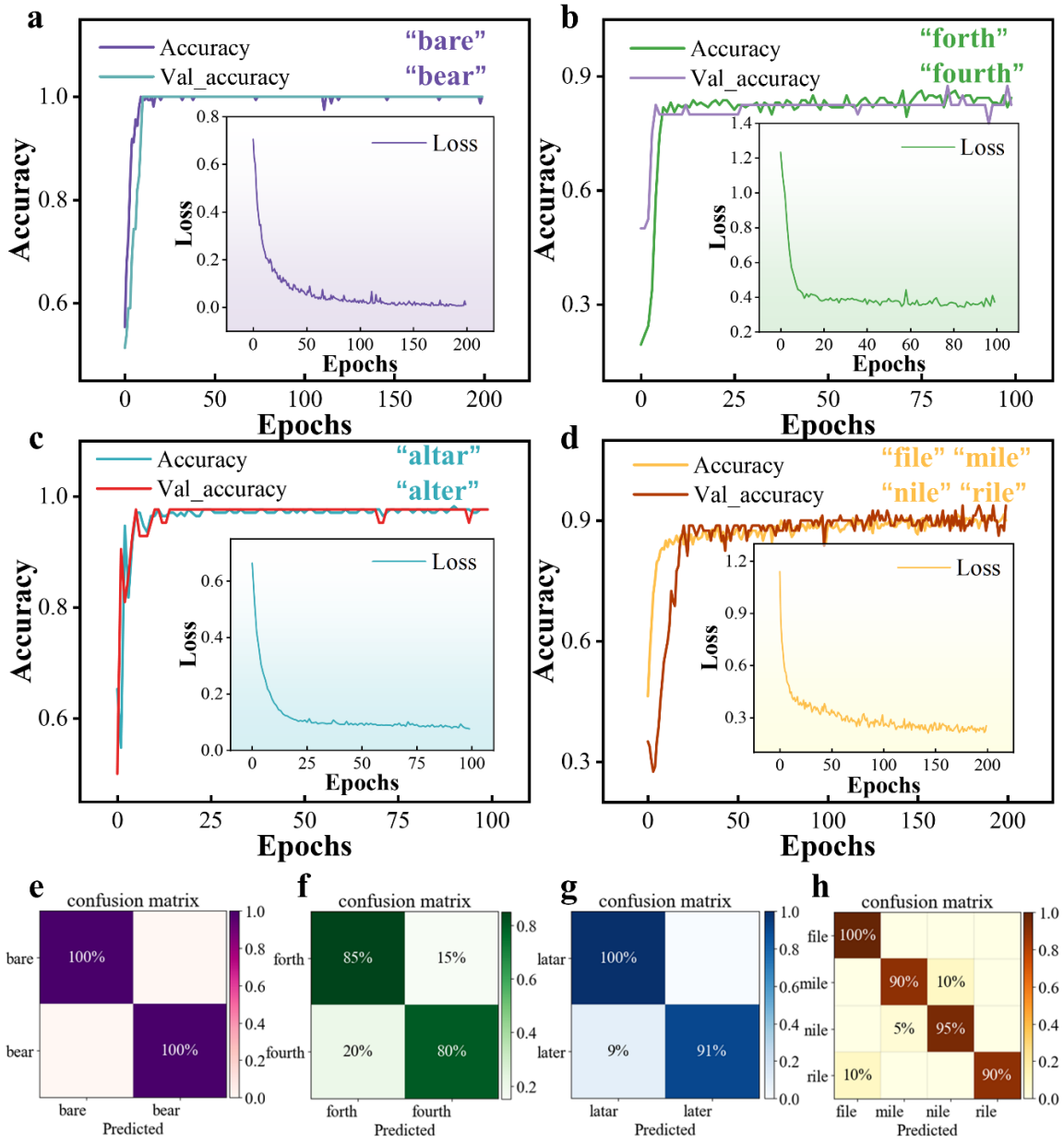

Figure 3. Recognition results of a series of slightly different words processed by handwriting recognition system. (a-d) Accuracy and loss curves for (a) identifying "bare" and "bear", (b) identifying "forth" and "fourth", (c) identifying "altar" and "alter", and (d) identifying "file", "mile", "nile" and "rile". **(e-h)** Confusion matrix to (e) identify "bare" and "bear", (f) identify "forth" and "fourth", (g) identify "altar" and "alter" and (h)

identify “file”, “mile”, “nile” and “rile”.

Our flexible handwriting recognition system can provide promising insights in the fields of human-machine interaction, for examples, playing electronic games, touching computer handwriting screen, and playing music (**Figure 4b**). To further demonstrate the potential application of the handwriting recognition system in constructing human-machine communication interfaces, we applied this system to play a piano. As shown in **Figure S9** and **Movie S1**, we demonstrated the process of playing the piano using the corresponding music through the system. Specifically, through the recognition of handwriting contents by the handwriting recognition system, and with the assistance of a clicker, the corresponding keys on the piano can be played to generate sounds. This can facilitate those music creators, who can detect the quality of music simply by writing the corresponding music scores. Similarly, various applications could be explored using the hydrogel handwriting recognition system, including playing electronic games and customizing routes for robots.

Furthermore, in this work, we applied the system for signature recognition. The components of the signature recognition system are shown in **Figure 4a.** A total of 690 handwritten signatures (e.g., OK) were acquired from 7 participants, as shown in **Figure S10**. After subsequent processing, the acquired signals were put into the BiLSTM model, as shown in **Figure 4c**. **Figures 4d** shows the performance of the system for signature recognition, with a recognition accuracy of 91.03% and a recognition time of less than 1s. The confusion matrix shown in **Figure 4e** demonstrates the high recognition accuracy of the constructed BiLSTM learning architecture for the custom signature dataset. The above result clearly demonstrates the prospect of our hydrogel handwriting recognition system for signature recognition. More applications can be extended to the encryptors, which utilize the ability of BiLSTM model to process and analyze sequential data, and thus realize the functions of information reading and writing, as well as further information encryption.

We believe that our handwriting system is a breakthrough for the application of hydrogel sensor.

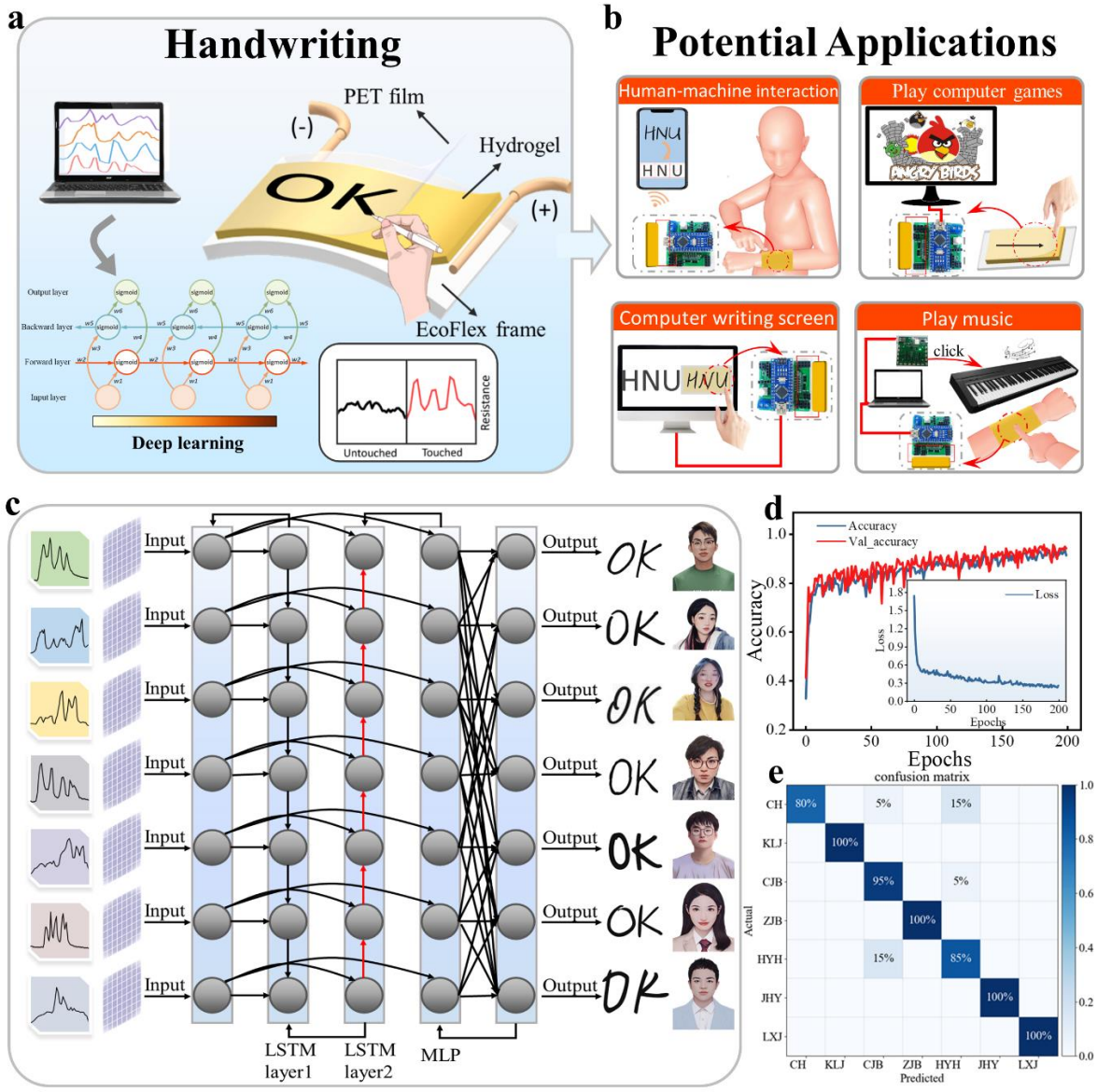

Figure 4. Demonstration of the flexible handwriting recognition system. (a-b) Schematic diagram of the composition of the hydrogel handwriting recognition system and its potential applications. **(c)** The process of signature recognition. **(d)** Accuracy and loss curves and **(e)** Confusion matrix for recognizing signature recognition of seven individuals.

5. CONCLUSIONS

In conclusion, we have developed a machine-learning assisted handwriting recognition using GO-based hydrogel for high-accuracy handwriting recognition. Our system offers a number of attractive features including high sensitivity, high stretchability, low weight, and low cost. The signals were collected through the GO hydrogel sensors, post-processed and then sent to the BiLSTM model for training. The system accurately recognized 26 letters and 10 number, with a high accuracy rate of over 90%. Additionally, we demonstrated that the system achieved a high accuracy for the recognition of similar words. Furthermore, we applied our handwriting recognition system for signature recognition, showing an accuracy rate of 91.30% and a recognition time of less than 1s. In particular, we also demonstrated playing music through hydrogel handwriting recognition system, proving its potential in constructing human-machine communication interfaces. We believe that this work not only proposes a practical strategy to construct machine-learning-assisted handwriting recognition system with a high accuracy, but also provides a new methodology for designing promising materials for flexible electronics.

6. METHODS

Materials. All chemical regents employed in this research were obtained commercially and used as received without further purification. Acrylamide (AAm, 99.0%), Dopamine hydrochloride (DA, 98%), ethanol (C_2H_5OH, ≥99.7%), calcium chloride ($CaCl_2$, 96.0%), *N,N′*-methylenebis-acrylamide (MBA, ≥99.0%), potassium persulfate (KPS, 99.5%), and *N,N,N′,N′*-tetramethylethylenediamine (TEMED, ≥99.5%) were purchased from Aladdin Ltd (Shanghai, China). Graphite oxide powders (0.5-5μm) was purchased from XFNANO Ltd (Nanjing, China). Ammonia hydroxide solution ($NH_3 \cdot H_2O$, 25.0~28.0%) was purchased from Macklin Ltd (Shanghai, China). Sodium casein (SC, ≥90%) was obtained from Zhejiang Yinuo Biological Technology Co., Ltd. Deionized water was used to prepare aqueous solutions.

Preparation of hydrogels. The conductive GO hydrogels were fabricated according

to our previous study.[33] Typically, certain amounts of AAm monomer, $CaCl_2$, SC, and PDA solution were firstly dissolved into deionized water, and then magnetically stirred for 20 min at 40 °C. The weight ratio of AAm, $CaCl_2$, SC, and PDA was 4:0.35:1:3. Then, the MBA crosslinker and GO dispersion were added into the mixed solution under N_2 atmosphere. The weight ratios of MBA/AAm and GO/AAm were set to be 0.001:2 and 0.001:1, respectively. After stirred for 30 min at room temperature, KPS (0.05 g) and TMEDA (50 μL) initiators were added to the mixture and stirred for 2 min at room temperature. Finally, the mixed solution was gently injected into a rectangular plastic mold and preserved at 40 ℃ for 2 h to achieve a gelation.

Characterization. The morphology of the GO nanosheets was examined using a transmission electron microscope (TEM, TF 20). Thickness of the GO nanosheets was measured using an atomic force microscope (AFM, Bruker Dimension ICON). Microstructures of the hydrogel samples after removal of solvent were obtained using a scanning electron microscope (SEM, TESCAN Company). The uniaxial tensile tests of the hydrogel samples (with a dimension of a length of 40 mm, a width of 20 mm, and a thickness of 5 mm) were performed using a mechanical testing machine (ZQ-990LB, 500 N, China) with a speed of 100 mm/min, and the clamping distance was set to be 5 mm. A source meter (Keithley 2611B) was used to measure the electrical signals of hydrogel stain sensors.

Data composition. For the specific composition of the data, our custom datasets were divided into different categories, including 26 categories of letters, 10 categories of numbers, 4 categories of similar words, and 7 categories of signatures. Each category contained about 100 samples.

Machine-learning algorithm. The principle of BiLSTM was utilized in this work.

The BiLSTM model is a combination of forward LSTM and backward LSTM. The LSTM model consists of input word (X), cell state (C_t), temporary cell state (C), hidden

layer state (h), forgetting gate (f), memory gate (i_t) and output gate (o_t). The calculation process of LSTM is following the selective filtering of the information through a well-designed "gate" structure. The hidden layer state (h) will be the output at each time step, in which forgetting gate (f), memory gate (i_t) and output gate (o_t) are controlled by the last hidden layer state (h_{t-1}) and the current input (X_t).

The forgetting gate (f), memory gate (i_t), current cell state (C_t), output gate (o_t) and current hidden layer state (h_t) are calculated using the following formulas, respectively.

$$f_t = \sigma(W_f \cdot [h_{t-1}, x_t] + b_f);$$

$$i_t = \sigma(W_i \cdot [h_{t-1}, x_t] + b_i),\ \widetilde{C_t} = tanh(W_C \cdot [h_{t-1}, x_t] + b_C);$$

$$C_t = f_t * C_{t-1} + i_t * \widetilde{C_t};$$

$$o_t = \sigma(W_o \cdot [h_{t-1}, x_t] + b_o),\ h_t = o_t * tanh(C_t)$$

For the BiLSTM model, in the forward layer, the forward calculation was performed from time 1 to time t, and the output of the forward hidden layer at each time was obtained and saved. Similarly, in the backward layer, the backward calculation was performed from time t to time 1, and the output of the backward hidden layer at each time was obtained and saved. Finally, the final output was obtained by combining the output results of the forward layer and the backward layer at the corresponding time. The mathematical expressions are as follows:

$$h_t = f(w_1 x_t + w_2 h_{t-1});$$

$$h'_t = f(w_3 x_t + w_5 h'_{t+1});$$

$$o_t = g(w_4 h_t + w_6 h'_t)$$

Supporting Information

- Figure S1. Photographic images demonstrating the stretchability of the GO hydrogel.
- Figure S2. The sensitivity curves of hydrogels with different compositions.
- Figure S3. The factors that affect the intensities and patterns of output signals.

- Figure S4. Demonstration of repeatability of the data obtained from handwriting recognition system.
- Figure S5. Results of 26 letters recognized by different machine learning models.
- Figure S6. Comparison of various parameters of 26 letters recognized by different convolution neural network models.
- Figure S7. Comparison of various parameters of 26 letters recognized by CNN and different recurrent neural network models.
- Figure S8. Visualizing the information from the datasets of letters and numbers using t-SNE dimensionality reduction.
- Figure S9. The demonstration of playing the piano through handwriting recognition system.
- Figure S10. The resistance variation of signature written by seven individuals.
- **Experimental platforms and hyperparameters of different models.**
- Table S1. The detailed experimental parameters of Lenet-5 model.
- Table S2. The detailed experimental parameters of AlexNet model.
- Table S3. The detailed experimental parameters of VGG16 model.
- Table S4. The detailed experimental parameters of ResNet model.
- Table S5. The detailed experimental parameters of CNN model.
- Movie S1 (MP4 format). The process of playing the corresponding music through hydrogel handwriting recognition system.

Conflicts of Interest

The authors declare no conflict of interest.

Author Contributions

The manuscript was written through contributions of all authors. All authors have given approval to the final version of the manuscript.

ACKNOWLEDGMENTS

This work was supported by the Excellent Youth Fund of Hunan Province (2021JJ20018), the NSFC (No. 52075162), the Program of New and High-tech Industry of Hunan Province (2020GK2015, 2021GK4014), the Joint Fund Project of the Ministry of Education, and the Engineering Physics and Science Research Council of UK (EPSRC EP/P018998/1) and International Exchange Grant (IEC/NSFC/201078) through Royal Society and the NSFCC.

REFERENCES

(1) Qu, X.; Liu, Z.; Tan, P.; Wang, C.; Liu, Y.; Feng, H.; Luo, D.; Li, Z.; Wang, Z. L. Artificial tactile perception smart finger for material identification based on triboelectric sensing. *Sci Adv* **2022**, *8* (31), eabq2521. DOI: 10.1126/sciadv.abq2521.

(2) Wang, M.; Wang, T.; Luo, Y.; He, K.; Pan, L.; Li, Z.; Cui, Z.; Liu, Z.; Tu, J.; Chen, X. Fusing Stretchable Sensing Technology with Machine Learning for Human–Machine Interfaces. *Adv Funct Mater* **2021**, *31* (39). DOI: 10.1002/adfm.202008807.

(3) Jung, Y. H.; Hong, S. K.; Wang, H. S.; Han, J. H.; Pham, T. X.; Park, H.; Kim, J.; Kang, S.; Yoo, C. D.; Lee, K. J. Flexible Piezoelectric Acoustic Sensors and Machine Learning for Speech Processing. *Adv Mater* **2020**, *32* (35), e1904020. DOI: 10.1002/adma.201904020.

(4) Wang, M.; Yan, Z.; Wang, T.; Cai, P.; Gao, S.; Zeng, Y.; Wan, C.; Wang, H.; Pan, L.; Yu, J.; et al. Gesture recognition using a bioinspired learning architecture that integrates visual data with somatosensory data from stretchable sensors. *Nature Electronics* **2020**, *3* (9), 563-570. DOI: 10.1038/s41928-020-0422-z.

(5)Wen, F.; Sun, Z.; He, T.; Shi, Q.; Zhu, M.; Zhang, Z.; Li, L.; Zhang, T.; Lee, C. Machine Learning Glove Using Self-Powered Conductive Superhydrophobic Triboelectric Textile for Gesture Recognition in VR/AR Applications. *Adv Sci (Weinh)* **2020**, *7* (14), 2000261. DOI: 10.1002/advs.202000261.

(6) Xue, J.; Zou, Y.; Deng, Y.; Li, Z. Bioinspired sensor system for health care and human-machine interaction. *EcoMat* **2022**, *4* (5). DOI: 10.1002/eom2.12209.

(7) Yao, H.; Li, P.; Cheng, W.; Yang, W.; Yang, Z.; Ali, H. P. A.; Guo, H.; Tee, B. C. K. Environment-Resilient Graphene Vibrotactile Sensitive Sensors for Machine Intelligence. *ACS Materials Letters* **2020**, *2* (8), 986-992. DOI: 10.1021/acsmaterialslett.0c00160.

(8) Sempionatto, J. R.; Moon, J. M.; Wang, J. Touch-Based Fingertip Blood-Free Reliable Glucose Monitoring: Personalized Data Processing for Predicting Blood Glucose Concentrations. *ACS Sens* **2021**, *6* (5), 1875-1883. DOI: 10.1021/acssensors.1c00139.

(9)Wen, F.; Zhang, Z.; He, T.; Lee, C. AI enabled sign language recognition and VR space bidirectional communication using triboelectric smart glove. *Nat Commun* **2021**, *12* (1), 5378. DOI: 10.1038/s41467-021-25637-w.
(10) Duan, S.; Lin, Y.; Zhang, C.; Li, Y.; Zhu, D.; Wu, J.; Lei, W. Machine-learned, waterproof MXene fiber-based glove platform for underwater interactivities. *Nano Energy* **2022**, *91*. DOI: 10.1016/j.nanoen.2021.106650.
(11) Cao, Y.; Yang, Y.; Qu, X.; Shi, B.; Xu, L.; Xue, J.; Wang, C.; Bai, Y.; Gai, Y.; Luo, D.; et al. A Self-Powered Triboelectric Hybrid Coder for Human-Machine Interaction. *Small Methods* **2022**, *6* (3), e2101529. DOI: 10.1002/smtd.202101529.
(12) Zhao, X.; Chen, X.; Yuk, H.; Lin, S.; Liu, X.; Parada, G. Soft Materials by Design: Unconventional Polymer Networks Give Extreme Properties. *Chem Rev* **2021**, *121* (8), 4309-4372. DOI: 10.1021/acs.chemrev.0c01088.
(13) Luo, X.; Zhu, L.; Wang, Y. C.; Li, J.; Nie, J.; Wang, Z. L. A Flexible Multifunctional Triboelectric Nanogenerator Based on MXene/PVA Hydrogel. *Adv Funct Mater* **2021**, *31* (38). DOI: 10.1002/adfm.202104928.
(14) Burdick, J. A.; Murphy, W. L. Moving from static to dynamic complexity in hydrogel design. *Nat Commun* **2012**, *3*, 1269. DOI: 10.1038/ncomms2271.
(15) Zhang, Y. S.; Khademhosseini, A. Advances in engineering hydrogels. *Science* **2017**, *356* (6337). DOI: 10.1126/science.aaf3627.
(16) Kweon, O. Y.; Samanta, S. K.; Won, Y.; Yoo, J. H.; Oh, J. H. Stretchable and Self-Healable Conductive Hydrogels for Wearable Multimodal Touch Sensors with Thermoresponsive Behavior. *ACS Appl Mater Interfaces* **2019**, *11* (29), 26134-26143. DOI: 10.1021/acsami.9b04440.
(17) Su, G.; Yin, S.; Guo, Y.; Zhao, F.; Guo, Q.; Zhang, X.; Zhou, T.; Yu, G. Balancing the mechanical, electronic, and self-healing properties in conductive self-healing hydrogel for wearable sensor applications. *Mater Horiz* **2021**, *8* (6), 1795-1804. DOI: 10.1039/d1mh00085c.
(18) Qin, Z.; Sun, X.; Yu, Q.; Zhang, H.; Wu, X.; Yao, M.; Liu, W.; Yao, F.; Li, J. Carbon Nanotubes/Hydrophobically Associated Hydrogels as Ultrastretchable, Highly Sensitive, Stable Strain, and Pressure Sensors. *ACS Appl Mater Interfaces* **2020**, *12* (4), 4944-4953. DOI: 10.1021/acsami.9b21659.
(19) Gao, G.; Yang, F.; Zhou, F.; He, J.; Lu, W.; Xiao, P.; Yan, H.; Pan, C.; Chen, T.; Wang, Z. L. Bioinspired Self-Healing Human-Machine Interactive Touch Pad with Pressure-Sensitive Adhesiveness on Targeted Substrates. *Adv Mater* **2020**, *32* (50), e2004290. DOI: 10.1002/adma.202004290.
(20) Ge, G.; Lu, Y.; Qu, X.; Zhao, W.; Ren, Y.; Wang, W.; Wang, Q.; Huang, W.; Dong, X. Muscle-Inspired Self-Healing Hydrogels for Strain and Temperature Sensor. *ACS Nano* **2020**, *14* (1), 218-228. DOI: 10.1021/acsnano.9b07874.
(21) Zhang, Y. Z.; Lee, K. H.; Anjum, D. H.; Sougrat, R.; Jiang, Q.; Kim, H.; Alshareef, H.

N. MXenes stretch hydrogel sensor performance to new limits. *Sci Adv* **2018**, *4* (6), eaat0098. DOI: 10.1126/sciadv.aat0098.
(22) Shit, A.; Heo, S. B.; In, I.; Park, S. Y. Mineralized Soft and Elastic Polymer Dot Hydrogel for a Flexible Self-Powered Electronic Skin Sensor. *ACS Appl Mater Interfaces* **2020**, *12* (30), 34105-34114. DOI: 10.1021/acsami.0c08677.
(23)Peng, H.; Xin, Y.; Xu, J.; Liu, H.; Zhang, J. Ultra-stretchable hydrogels with reactive liquid metals as asymmetric force-sensors. *Materials Horizons* **2019**, *6* (3), 618-625. DOI: 10.1039/c8mh01561a.
(24) Pan, X.; Wang, Q.; Guo, R.; Ni, Y.; Liu, K.; Ouyang, X.; Chen, L.; Huang, L.; Cao, S.; Xie, M. An integrated transparent, UV-filtering organohydrogel sensor via molecular-level ion conductive channels. *Journal of Materials Chemistry A* **2019**, *7* (9), 4525-4535. DOI: 10.1039/c8ta12360h.
(25) Wang, C.; Li, J.; Fang, Z.; Hu, Z.; Wei, X.; Cao, Y.; Han, J.; Li, Y. Temperature-Stress Bimodal Sensing Conductive Hydrogel-Liquid Metal by Facile Synthesis for Smart Wearable Sensor. *Macromol Rapid Commun* **2022**, *43* (1), e2100543. DOI: 10.1002/marc.202100543.
(26) Tan, P.; Han, X.; Zou, Y.; Qu, X.; Xue, J.; Li, T.; Wang, Y.; Luo, R.; Cui, X.; Xi, Y.; et al. Self-Powered Gesture Recognition Wristband Enabled by Machine Learning for Full Keyboard and Multicommand Input. *Adv Mater* **2022**, *34* (21), e2200793. DOI: 10.1002/adma.202200793.
(27) Minglu Zhu1, 3,4, Zhongda Sun1,2,3, Zixuan Zhang1,2,3, Qiongfeng Shi1,2,3, Tianyiyi He1,2,3,4, Huicong Liu5, Tao Chen5*, Chengkuo Lee1,2,3,4,6*. Haptic-feedback smart glove as a creative human-machine interface (HMI) for virtualaugmented reality applications. *SCIENCE ADVANCES*.
(28) Liu, S.; Zhang, J.; Zhang, Y.; Zhu, R. A wearable motion capture device able to detect dynamic motion of human limbs. *Nat Commun* **2020**, *11* (1), 5615. DOI: 10.1038/s41467-020-19424-2.
(29) Zhou, Z.; Chen, K.; Li, X.; Zhang, S.; Wu, Y.; Zhou, Y.; Meng, K.; Sun, C.; He, Q.; Fan, W.; et al. Sign-to-speech translation using machine-learning-assisted stretchable sensor arrays. *Nature Electronics* **2020**, *3* (9), 571-578. DOI: 10.1038/s41928-020-0428-6.
(30) Sun, Z.; Zhu, M.; Zhang, Z.; Chen, Z.; Shi, Q.; Shan, X.; Yeow, R. C. H.; Lee, C. Artificial Intelligence of Things (AIoT) Enabled Virtual Shop Applications Using Self-Powered Sensor Enhanced Soft Robotic Manipulator. *Adv Sci (Weinh)* **2021**, *8* (14), e2100230. DOI: 10.1002/advs.202100230.
(31) Huang, J.; Gu, J.; Liu, J.; Guo, J.; Liu, H.; Hou, K.; Jiang, X.; Yang, X.; Guan, L. Environment stable ionic organohydrogel as a self-powered integrated system for wearable electronics. *Journal of Materials Chemistry A* **2021**, *9* (30), 16345-16358. DOI: 10.1039/d1ta03618a.
(32) Wu, M.; Pan, M.; Qiao, C.; Ma, Y.; Yan, B.; Yang, W.; Peng, Q.; Han, L.; Zeng, H.

Ultra stretchable, tough, elastic and transparent hydrogel skins integrated with intelligent sensing functions enabled by machine learning algorithms. *Chem. Eng. J.* **2022**. DOI: 10.1016/j.cej.2022.138212.
(33) Zhou, J.; Zhuo, F.; Long, X.; Liu, Y.; Lu, H.; Luo, J.; Chen, L.; Dong, S.; Fu, Y.; Duan, H. Bio-inspired, super-stretchable and self-adhesive hybrid hydrogel with SC-PDA/GO-Ca2+/PAM framework for high precision wearable sensors. *Chem. Eng. J.* **2022**, *447*. DOI: 10.1016/j.cej.2022.137259.